






Design and Construction of the New 85T Duplex Magnet at NHMFL-Los Alamos

James R. Michel , Scott B. Betts , Jason D. Lucero, Ashish Bhardwaj , *Senior Member, IEEE*,
Linh N. Nguyen , and Doan N. Nguyen 

Abstract—The National High Magnetic Field Laboratory’s Pulsed Field Facility at Los Alamos National Laboratory develops and provides ultra-high pulsed magnetic fields for scientific research. The facility houses several types of non-destructive pulsed magnets which can deliver the peak fields ranging from 60 T to 100 T for users. Two flagship magnets are the 100-T Multi-shot (100TMS) pulsed magnet and the 60-T Long Pulsed (60TLP) magnet, and both magnets are primarily driven by the powerful 1.4 GW generator. These two flagship magnets have been offline since 2019 while the generator was disassembled for program specific rotor upgrade and maintenance. To partially fulfill the strong demand from users to access higher magnetic fields, a new capacitor driven magnet system, the 85-T duplex (85TD) magnet, was recently developed. The 85TD magnet cannot match the magnetic field amplitude of the signature 100TMS generator driven magnet but can deliver 20 Tesla higher than the peak field of the workhouse 65-T short-pulsed magnets. This article will report technical design, construction, and possible risks associated with operation of the 85TD magnet.

Index Terms—Duplex magnet, finite element modeling, high magnetic field, pulsed magnet.

I. INTRODUCTION

THE National High Magnetic Field Laboratory (NHMFL)’s Pulsed Field Facility (PFF) is located and operated by the Los Alamos National Laboratory (LANL) in New Mexico. The facility houses powerful multi-shot pulsed magnets to provide pulsed magnetic fields ranging from 65 T to 100 T for users [1], [2]. Notably, PFF built and operated two signature pulsed magnet systems, the 60-T Long Pulsed (60TLP) [3], [4] magnet and the 100-T multi-shot (100TMS) magnet [5], [6]. Both are driven primarily by the powerful 1 GJ-1.4 GW generator. However, these two flagship magnets have been offline since 2019 while the generator was disassembled for program specific rotor upgrade and maintenance. PFF promptly built two new magnets to partially fill the demand of users for longer pulses and higher fields than our standard 65-T user magnets can provide. These magnets are the 60-T mid-pulsed (60TMP) magnet and

Manuscript received 25 September 2023; revised 18 November 2023 and 21 November 2023; accepted 22 November 2023. Date of publication 6 December 2023; date of current version 18 December 2023. This work was supported in part by NSF through NHMFL under Grants DMR-1157490 and DMR-1644779, and in part by DoE through LANL. (*Corresponding author: Doan N. Nguyen.*)

The authors are with the Los Alamos National Laboratory, Los Alamos, NM 87544 USA (e-mail: doan@lanl.gov).

Color versions of one or more figures in this article are available at <https://doi.org/10.1109/TASC.2023.3338580>.

Digital Object Identifier 10.1109/TASC.2023.3338580

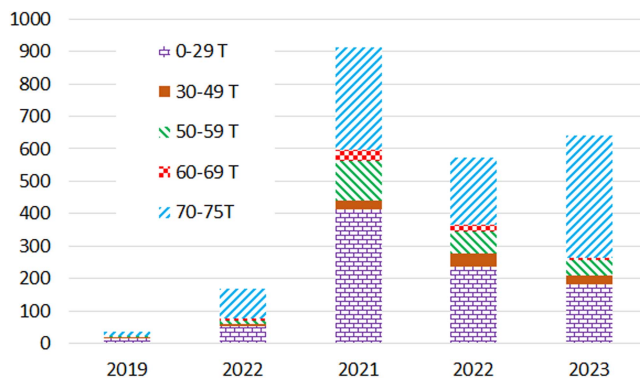


Fig. 1. Pulse statistics of 75T duplex magnet after several years of service to users.

75-T Duplex (75TD) magnet [7], [8]. Both 60TMP and 75TD magnets have been used extensively by users since they were commissioned. For instance, Fig. 1 shows the performance and pulse statistics of the 75TD magnet since it was commissioned in late 2019 to the middle of 2023. During this time, 75TD magnet has delivered nearly 1000 pulses of magnetic fields between 73–75 T, resulting in numerous high-quality scientific papers published in the last several years. Based on the success of the 75TD magnet and requests for higher fields, the 85 T Duplex magnet (85TD) has been designed and constructed.

II. DESIGN AND CONSTRUCTION OF 85-T DUPLEX MAGNET

A. Specification and Field Profile of 85TD Magnet

The use of multiple nested coils driven by independent capacitor banks has been an effective and safer approach to produce ultra-high pulsed magnetic fields at different pulsed field facilities [8], [9], [10], [11], [12]. The two capacitor banks available at LANL’s PFF have been used to power a new 85-T duplex magnet and Table I summarizes the specification of that magnet. The magnet bore is 10.5 mm, the same size as our 100TMS magnet. The inner coil of the 85TD magnet is driven by 2.3 MJ of energy drawn from 2.5 MJ-18 kV capacitor bank. The coil is constructed of 8 layers of 3×5.8 mm CuNb wire of which mechanical and electrical properties were given in [13]. The outer coil is a monolithically wound 8 layers of 4×5.5 mm glidcop AL15 wire. The tensile strength of the glidcop AL15 wire is about 600 MPa at 77 K and 480 MPa at room temperature. This coil is designed to be driven by about 3 MJ of energy drawn from our

TABLE I
SPECIFICATION OF 85TD MAGNET

Specification	
Inner coil winding	8 layers of CuNb (3 x 5.8 mm)
Outer coil winding	6 layers of Glidcop AL15
Maximum energy	5.3 MJ
Peak training field	86 T
Peak field for user	84 T
Bore size	10.5 mm (same as 100T magnet)

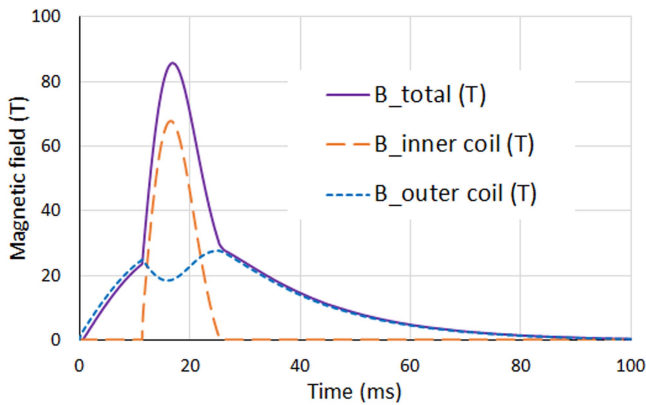


Fig. 2. Profiles of contributed magnetic fields from the inner and outer coils and the total magnetic field.

4 MJ-16 kV capacitor bank. The total energy needed to drive the 85TD magnet is about 5.3 MJ. Fig. 2 plots the waveforms of magnetic fields generated by the component coils and the total field in the bore of the magnet. At the peak magnetic field, the inner coil generates 68 T in the 18 T background field generated by the outer coil to deliver the peak magnetic field of 86 T. The pulse length of the magnetic field generated by the inner coil is 13 ms and the pulse length of magnetic field generated by the outer coil is about 100 ms.

B. Mechanical Performance of 85TD Magnet

Similar to the designs of our high field pulsed magnets, the 85TD magnet design relied heavily on Zylon fiber [14] and MP35N [15] to provide the reinforcement for the windings. Zylon fiber must be applied at high tension to compensate for its negative thermal expansion when the magnet is cooled for a pulse [14]. Fig. 3 depicts the distribution of the peak von Mises stresses in the mid-plane of the 85TD magnet. For comparison, similar von Mises stress distribution for the windings of the insert coil of our flagship 100-T magnet is also plotted in that figure. Generally, stress in the windings of the 85TD magnet are slightly lower than those in the 100-T insert coil. The maximum stress in the winding of 100-T insert coil reach 2.7 GPa while the maximum stress in winding of 85TD magnet reaches 2.6 GPa. With a high Young's Modulus, Zylon fiber takes a large fraction of hoop loads and experiences the highest stress in both magnets.

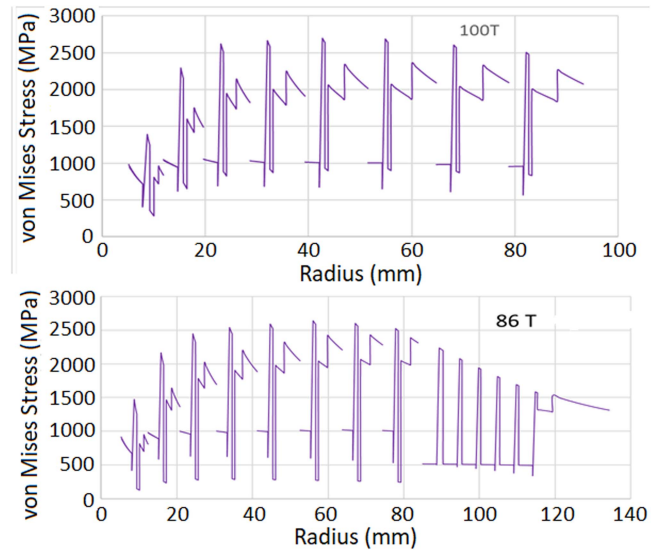


Fig. 3. Mid-plane von Mises stress at the peak magnetic field for the insert of 100T magnet (top) and the new 85TD magnet (bottom).

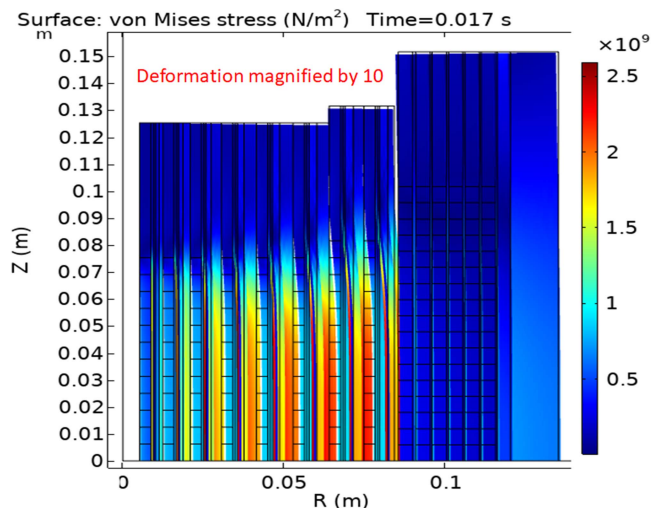


Fig. 4. von Mises stress distributed over the winding cross-section of the 85TD magnet when magnetic field reaches the peak value of 86 T.

The conductor and MP35N experience lower stress levels. For the 85TD magnet, the maximum stress in the CuNb conductor of inner coil reaches about 1 GPa while the maximum stress in MP35N reaches about 2 GPa.

To study mechanical performance for the entire winding cross-section, finite element analysis (FEA) simulations are used. Details on our comprehensive, multi-engineering FEA models for pulsed magnet design can be found in [16]. Fig. 4 depicts the von Mises stress distribution over the cross-section of the magnet at the peak magnetic field. The peak stresses in the zylon layers reach about 2.6 GPa, nearly the same stress at the mid-planes shown in Fig. 3, which was obtained by our standard Pulsed Magnet Design Code [17]. Fig. 5 plots the distribution of the axial stress over the windings of the 85TD magnet. Generally, most of the winding regions experience compressive stresses

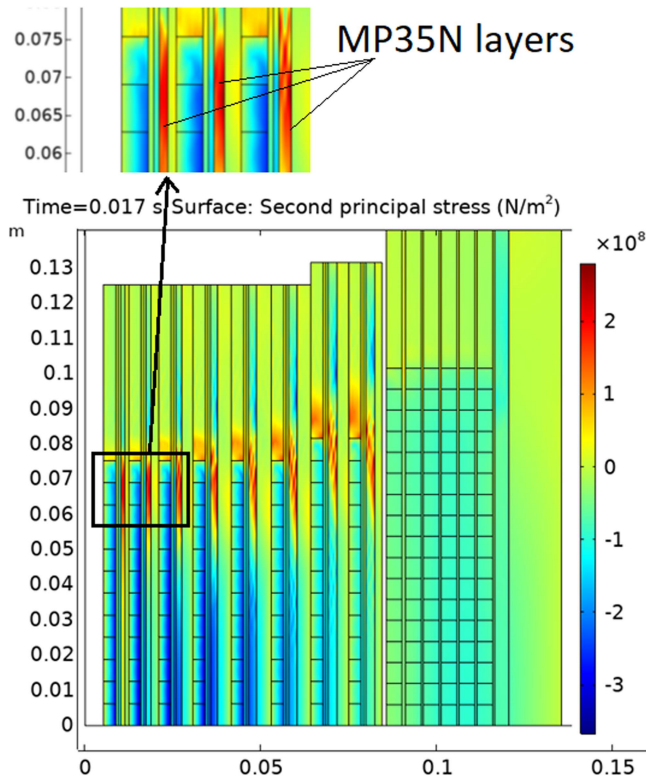


Fig. 5. Axial stress distributed over the winding cross-section of the 85TD magnet when magnetic field reaches the peak value of 86 T.

caused by the radial magnetic field component near the ends of the windings. The maximum compressive stress of up to about 360 MPa, happens in layers 3, 4 and 5 of the inner coil. It is worth noting that the MP35N reinforcing layers also experience tensile stress near the winding ends. It is well-known that the hoop load is significantly reduced when the windings come to the end turns. At the junction between the conductor winding and the G10 end-spools, the hoop load even drops from hundreds of MPa in the last winding turn to nearly zero of very low hoop stress in the G10 end-spools. The high gradient of the hoop loads at the winding end regions caused the tensile stresses in those regions. Most of these axial tensile stresses are taken by the MP35N layers as seen in the insert of Fig. 5. The maximum tensile stress reaches 260 MPa, well below the UTS of MP35N metal shells. Therefore, MP35N layers are needed to bear that axial tensile load and prevent possible cracks of the Zylon fiber composite.

C. Thermal Performance of 85TD Magnet

The magnet is immersed in a liquid Nitrogen bath; thus, the temperature of the magnet winding is about 76 K prior to the pulse. The conductors of the inner coil are heated significantly during and at the end of the pulses as seen in Figs. 6 and 7 which depict temperature rises in the winding during an 86 T pulse calculated by the FEA simulations [16]. The eddy current effect was taken into account in the FEA simulations and it may cause quite non-uniform temperature rise in the winding near the beginning of the pulse as reported in [16]. However,

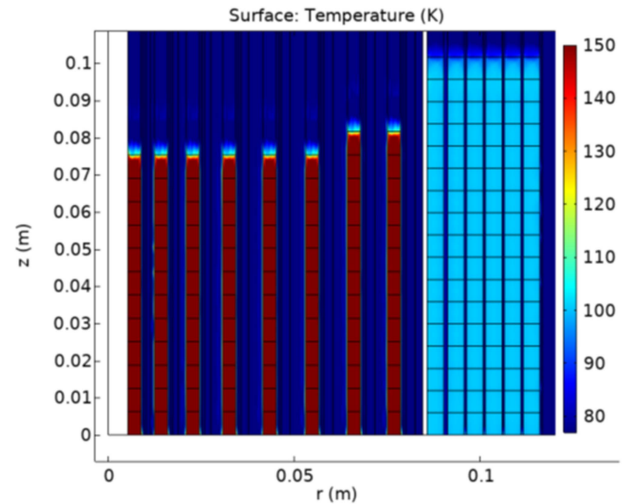


Fig. 6. Temperature rise in the winding of the 85T duplex magnet when magnetic field reaches the peak value of 86 T.

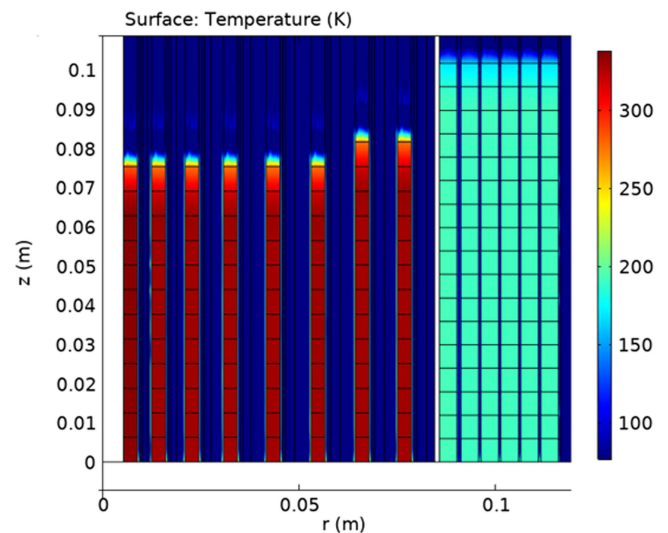


Fig. 7. Temperature rise in the winding of the 85T duplex magnet at the end of the pulse.

when the driving current is high enough and dB/dt is lower, the current distribution becomes uniform causing a quite uniform temperature rises. Fig. 6 shows that, at the peak magnetic field, the temperature of the inner coil winding increases to 150 K and temperature of the outer coil winding increases to 105 K. At the end of the pulse, the temperature of the winding of the inner coil reaches 340 K and temperature of the outer coil winding reaches 180 K, as seen in Fig. 7. These temperature rises are not high enough to soften the epoxy and should not impact the winding of the magnets. However, impact of temperature rises on the mechanical and electrical properties of materials must be carefully considered to accurately simulate the electromagnetic and mechanical performances of the magnet.

D. Construction and Installation of 85TD Magnet

The magnet has been built and installed in an upgraded blast box as seen in Fig. 8. The housing is designed to contain a 5 MJ



Fig. 8. Picture of 85T duplex magnet and its power delivery fixture mounted inside a strong G-10 blast-box.

catastrophic failure in the worse scenario. It is built from NEMA G10 sheets of 2-in thick with custom stainless-steel hinges and joints. The blast-box allows convenient access to the magnet system while protecting the users and experimental equipment from the high voltage of the power distribution components.

III. RISK ASSESSMENT AND MITIGATION

Two nested coils in the duplex design are driven by two independent capacitor banks. The strong transformer coupling between two coils can pose some serious risks if one of the coils does not operate correctly or as designed. We investigated two scenarios to identify the associated risks and provide solutions to prevent possible damages caused by these risks.

A. Outer Coil is Fired and the Inner Coil is Mis-Fired

In this scenario, the Silicon Controlled Rectifier (SCR) switch for the inner coil does not close due to a possible faulty control. When this fault happens, the electrical circuit of the inner coil is open and there is no current running in this coil. In this case, the outer coil will operate at higher current and produce higher magnetic field compared to the normal operation [11]. As a result, the stress in the outer coil winding will be higher during the fault. Fig. 9 plots the von Mises and hoop stresses in the winding of the 85TD magnet when the inner coil is mis-fired. The stress in winding of the inner coil is very small, mainly generated by pre-tensioned Zylon fibers and the Lorentz forces applying on the induced currents circulating in the MP35N metal reinforcements. However, the von Mises stress in the outer coil reaches 2.5 GPa, quite higher than the maximum stress of 2.2 GPa in that coil during normal operation. The stress level of 2.5 GPa during the fault is manageable and should not damage the magnet.

Induced voltage generated in the inner coil due to the transformer effect is plotted in Fig. 10. That voltage will be applied on the open terminals of the SCR switch. In this faulty condition, the

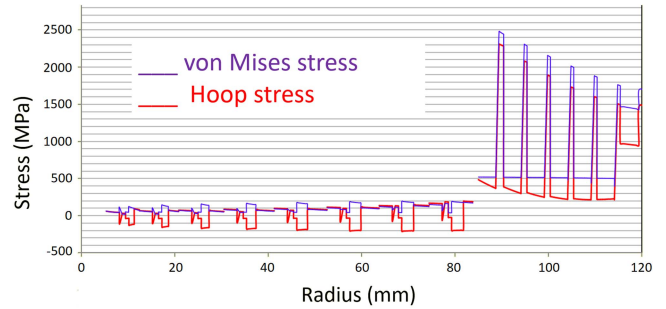


Fig. 9. Maximum von Mises and hoop stresses at the mid-plane along the magnet radius when the inner coil is mis-fired.

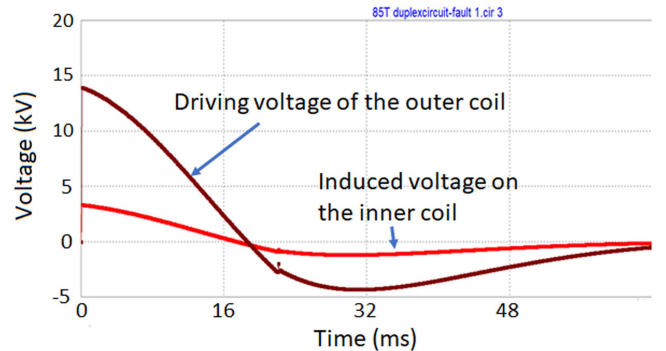


Fig. 10. Driving voltage of the outer coil and the induced voltage on the inner coil when the inner coil is mis-fired.

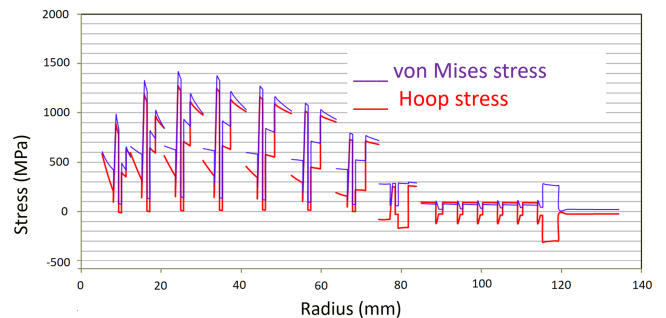


Fig. 11. Maximum von Mises and hoop stresses at the mid-plane along the magnet radius when the outer coil is mis-fired.

induced voltage reach 3.5 kV, well below the designed limit of our SCR switches and therefore no overload protection solution is needed.

B. Inner Coil is Fired and the Outer Coil is Mis-Fired

In the case that the outer coil is mis-fired, the stress over entire winding of the magnet is very low as seen in Fig. 11. Without the background magnetic field generated by the outer coil, the maximum von Mises stress in the inner coil is only 1.4 GPa, much lower than the peak stress of 2.6 GPa in that coil during normal operation.

While stress is low and not an issue, a very high induced voltage can be generated on the open outer coil as seen in Fig. 12. The driving voltage of the inner coil is 14 kV and can produce an induced voltage of about 24 kV on the outer coil. That voltage

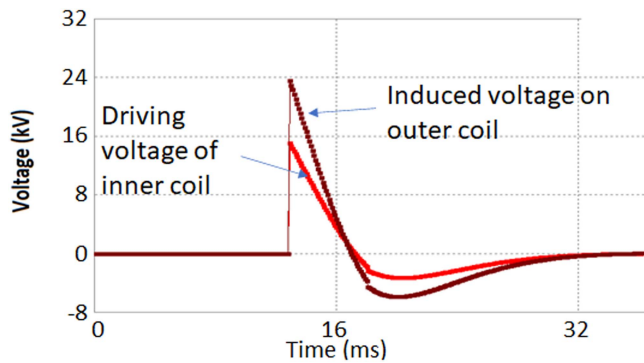


Fig. 12. Driving voltage of the inner coil and the induced voltage on the outer coil when the outer coil is mis-fired.

could damage its SCR switch, which is designed to operate up to 16 kV. Therefore, a bank of Metal Oxide Varistors (MOV) with a threshold voltage of 15 kV was built and connected in parallel to the outer coil to limit the induced voltage on the outer coil and protect its SCR switch from overloaded voltage. A similar protection approach has been developed for our 75 T duplex magnet [8] and its effectiveness to mitigate the risk of overloaded voltage was proofed.

V. CONCLUSION

Newly developed 60TMP and 75TD magnets at LANL's PFF have been used extensively by users. To better serve the requests from users for higher magnetic fields during the 100TMS magnet being temporarily offline, a new 85TD magnet has been designed and built. A total energy of 5.3 MJ from two capacitor banks will be used to train the magnet up to 86 T. Then a lower magnetic field, up to 84 T will be provided to users. At 86 T field, the maximum stress in the magnet winding reaches 2.6 GPa and the magnet should deliver at least 500 full-field pulses at that stress level. The windings of the inner coil will be heated to 340 K at the end of a full-field pulse. Generally, the stress level in the winding of the magnet is manageable during possible faults, but a MOV bank with a threshold voltage of 15 kV is required to be connected to the outer coil to limit the induced voltages on the terminals of that coil and therefore protect expensive SCR switches from the overloaded voltages.

ACKNOWLEDGMENT

Authors would like to thank Ke Han and other members of the magnet material team at the NHMFL in Tallahassee, Florida for their support in development and characterization of key materials used our pulsed magnets.

REFERENCES

- [1] D. N. Nguyen, J. Michel, and C. H. Mielke, "Status and development of pulsed magnets at the NHMFL pulsed field facility," *IEEE Trans. Appl. Supercond.*, vol. 26, no. 4, Jun. 2016, Art. no. 4300905.
- [2] C. A. Swenson et al., "Pulse magnet development program at NHMFL," *IEEE Trans. Appl. Supercond.*, vol. 14, no. 2, pp. 1233–1236, Jun. 2004.
- [3] J. R. Sims et al., "The US-NHMFL 60 T long pulse magnet failure," *IEEE Trans. Appl. Supercond.*, vol. 12, no. 1, pp. 480–483, Mar. 2002.
- [4] J. Schillig et al., "Operating experience of the United States National High Magnetic Field Laboratory 60 T long pulse magnet," *IEEE Trans. Appl. Supercond.*, vol. 10, no. 1, pp. 526–529, Mar. 2000.
- [5] J. Bacon et al., "The US-NHMFL 100 Tesla multi-shot magnet," *IEEE Trans. Appl. Supercond.*, vol. 12, no. 1, pp. 695–698, Mar. 2002.
- [6] M. Jaime et al., "Magnetostriction and magnetic texture to 100.75 Tesla in frustrated $\text{SrCu}_2(\text{BO}_3)_2$," *Proc. Nat. Acad. Sci.*, vol. 109, no. 31, pp. 12404–12407, Jul. 2012.
- [7] J. R. Michel, D. N. Nguyen, and J. D. Lucero, "Design, construction, and operation of new duplex magnet at pulsed field facility-NHMFL," *IEEE Trans. Appl. Supercond.*, vol. 30, no. 4, Jun. 2020, Art. no. 0500105.
- [8] Q. V. M. Nguyen, L. Torres, and D. N. Nguyen, "Electromagnetic interaction between the component coils of multiplex magnets," *IEEE Trans. Appl. Supercond.*, vol. 28, no. 3, Apr. 2018, Art. no. 4300804.
- [9] K. Kindo, "New pulsed-magnets for 100 T, long-pulse and diffraction measurements," *J. Phys.: Conf. Ser.*, vol. 51, 2006, Art. no. 522.
- [10] T. Peng et al., "Design and performance of the first dual coil magnet at the WHMFC," *J. Low Temp. Phys.*, vol. 170, no. 5, pp. 463–468, 2013.
- [11] J. Béard et al., "Design and tests of the 100-T triple coil at LNCMI," *IEEE Trans. Appl. Supercond.*, vol. 28, no. 3, Apr. 2018, Art. no. 4300305.
- [12] S. Zherlitsyn, B. Wustmann, T. Herrmannsdörfer, and J. Wosnitza, "Magnet technology development at the Dresden High Magnetic Field Laboratory," *J. Low Temp. Phys.*, vol. 170, pp. 447–451, 2013.
- [13] K. Han, V. J. Toplosky, R. Walsh, C. Swenson, B. Lesch, and V. I. Pantsyrnyi, "Properties of high strength CuNb conductor for pulsed magnet applications," *IEEE Trans. Appl. Supercond.*, vol. 12, no. 1, pp. 1176–1180, Mar. 2002.
- [14] R. P. Walsh and C. A. Swenson, "Mechanical properties of Zylon/Epoxy composite at 295 K and 77 K," *IEEE Trans. Appl. Supercond.*, vol. 16, no. 2, pp. 1761–1764, Jun. 2006.
- [15] K. Han et al., "Mechanical properties of MP35N as a reinforcement material for pulsed magnets," *IEEE Trans. Appl. Supercond.*, vol. 12, no. 1, pp. 1244–1247, Mar. 2002.
- [16] D. N. Nguyen and D. T. Vo, "Comprehensive finite element modeling for pulsed magnet design using COMSOL and Java," *IEEE Trans. Appl. Supercond.*, vol. 30, no. 4, Jun. 2020, Art. no. 4900605.
- [17] Y. M. Eyssa and P. Pernambuco-Wise, "Electrical thermal and mechanical modeling of pulsed magnets," NHMFL, Tallahassee, FL, USA, NHMFL's Intern. Rep., Jan. 1995.